

## Article

## Characterization of Phase Separated Structure and Interface in SBR/NBR blend by AFM and DSC

Junhyeok Jang<sup>a</sup>, Masayuki Kawazoe<sup>b</sup>, Hirohisa Yoshida<sup>\*a,c</sup>

<sup>a</sup> Department of Applied Chemistry, Graduate School of Urban Environmental Science, Tokyo Metropolitan University, Hachioji, Tokyo JAPAN

<sup>b</sup> Yokohama Rubber Co. Ltd., Hiratsuka, Kanagawa JAPAN

<sup>c</sup> JASRI/SPring-8, Sayou-cho, Hyogo JAPAN

\*yoshida-hirohsa@tmu.ac.jp

(Received October. 10, 2011; Accepted November. 21, 2011)

The interface of phase separated structure of styrene butadiene rubber (SBR) / acrylonitrile butadiene rubber (NBR) prepared by spin-coating from toluene and tetrahydrofuran (THF) solutions has been characterized by Atomic Force Microscopy (AFM) and Differential Scanning Calorimetry (DSC). AFM line profiles of the phase difference images have given the average thickness of the interface of SBR and NBR blends. On the other hand, the volume fraction of the interface has been evaluated from the heat capacity jump at glass transition of each polymer using DSC. By comparing those results, it has been suggested that the interface thickness of SBR/NBR blends depends on the size of phase separated domains and kinds of solvent. These results suggest that the dispersion state of SBR and NBR in each solution influenced the phase separated structure and the interface thickness.

Keywords: SBR/NBR blend, Phase separated structure and Interface, Atomic Force Microscopy

### 1. Introduction

Polymer blends are widely used in rubber industry to set of advantages of each polymer component without time-consuming new polymer synthesis proves. Most of the blends are thermodynamically immiscible because of the long chained molecular nature. In addition, the polar difference of the polymers, like an oil resistant rubber compound consisting of SBR and NBR, accelerates the phase separation. Consequently, the interface, which has poor physic-chemical interaction, becomes mechanically weak.

To fix the weakness of the interface caused immiscible polymer blends and maintain suitable phase separated morphology, compatibilizers are often used. When a proper block or graft copolymer is added to an immiscible blend system, the phase separation structure becomes finer and the interface thicker, then the physical properties is improved<sup>1)</sup>. On the other hand, the morphology of a blend also is affected by the way of mixing. Dry mixing is industrially preferable but from a scientific view point, solution mixing is also interesting to obtain various phase separated morphologies which cause characteristic physical properties<sup>2,3)</sup>.

Phase separated morphologies of polymer blends are investigated by microscopic method<sup>4)</sup>, scattering methods<sup>5,6)</sup> and thermal analysis<sup>7,8)</sup>. However, the investigation methods for the interface are limited because the interface existed inside of materials. In this study, styrene butadiene rubber (SBR) and acrylonitrile butadiene rubber (NBR) blend system mixing without any compatibilizer but via solution mixing with toluene or THF was carried out. The morphologies of SBR/NBR blends were observed by Atomic Force Microscope (AFM) and the interface thickness between phase separated SBR and NBR domains was determined. At the same time, the volume fraction

of the interfaces was determined by DSC and the results were compared to those of AFM measurement.

### 2. Experimental

#### 2.1 Samples and preparations

The rubbers used in this study were styrene butadiene rubber (SBR; 23.5 % of styrene content, density 0.94 g/cm<sup>3</sup>, Solubility parameter SP = 17 MPa<sup>1/2</sup>, Nipol 1502 ZEON Co., Japan) and acrylonitrile butadiene rubber (NBR; 33.5 % of acrylonitrile content, density 0.98 g/cm<sup>3</sup>, SP = 19.9 MPa<sup>1/2</sup>, Nipol 1042 ZEON Co.). SBR/NBR blend samples were prepared by spin-coating from 4 wt% of rubber in toluene (SP = 18.2 MPa<sup>1/2</sup>), or tetrahydrofuran (THF, SP = 18.6 MPa<sup>1/2</sup>), solutions. The polymer weight fraction of SBR in the blend samples ( $\phi_{\text{SBR}}$ ) was varied as 0.3, 0.5, and 0.7 wt%.

#### 2.2 Measurements

SBR/NBR blends for AFM observation were prepared by spin-coating at 1000 rpm on silicon wafer from 4wt% toluene and THF solutions, and were dried under vacuum for 24 hours at room temperature. The AFM observation was performed by dynamic force mode at room temperature using E-sweep (SII Nanotechnology Inc., JAPAN). The spring constant of the cantilever and the measurement frequency were 37 N/m and 297 kHz respectively.

DSC measurement of SBR/NBR blends was performed by DSC7020 (SII Nano Technology Inc., JAPAN) equipped with cooling apparatus at 5 K/min in the temperature range from 130 to 480 K under nitrogen flow atmosphere.

Phase diagrams of SBR/NBR solution were created from 4 wt% of rubber in toluene and THF solution at 0.3, 0.5 and 0.7 of  $\phi_{\text{SBR}}$  at room temperature. After mixing the solutions, each

solution was kept for one week at room temperature until obtaining two layers separation. The volume of upper and lower layer was determined by measuring the layer length in the test tube and the fraction of solvent in upper and lower layers was determined by weight loss after spin-coating. The fraction of SBR and NBR in solid polymers prepared by casting was determined by Fourier transfer infrared spectroscopy measurement.

### 3. Results and discussion

#### 3.1 AFM observation

SBR/NBR blends showed macroscopic phase separation like a sea and islands structure in  $\mu\text{m}$  scale by optical microscopy. The sphere like domains (islands) dispersed heterogeneously in the matrix (sea), and those sizes were less than  $20\ \mu\text{m}$  with bimodal size distribution. Fig. 1 shows AFM phase images in  $30\ \mu\text{m} \times 30\ \mu\text{m}$  scale for SBR/NBR blends with various SBR fractions ( $\phi_{\text{SBR}}$ ) prepared from toluene and THF solutions. The micro scale domains in the size less than  $3\ \mu\text{m}$  were observed in all SBR/NBR blends. The macro domains with the diameters over  $10\ \mu\text{m}$  contained micro domains with the diameters less than  $1\ \mu\text{m}$ . This phenomenon suggests that the observed phase separated structure is the transient state to form the equilibrium phase separation.

In AFM phase image, a small phase angle means stiff part of lower energy absorption between sample and cantilever. That part corresponds to NBR rich phase in SBR/NBR blend systems used in this study because the dynamic modulus of NBR (0.56 Pa) is higher than that of SBR (0.32 Pa) at room temperature by Dynamic Mechanical Analysis (DMA). In Fig.1, the white and the dark parts indicate SBR and NBR rich phases respectively. The phase separation structure of SBR/NBR blends prepared from toluene solutions always consists of NBR rich domains and SBR rich matrix. Even for the system with 0.3 of  $\phi_{\text{SBR}}$ , the NBR rich phase had round and non-round domains in SBR rich matrix. On the other hand, the matrix changed from SBR to NBR for SBR/NBR blends prepared from THF solution in the case of  $\phi_{\text{SBR}}$  range below 0.5.

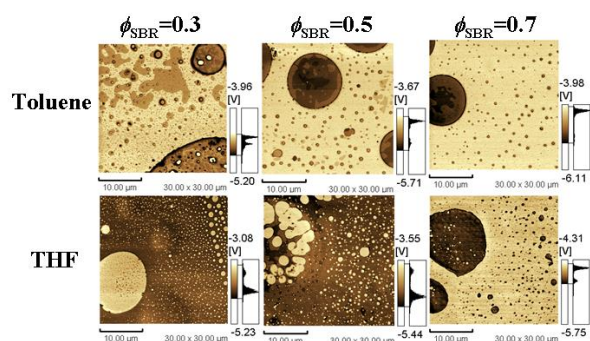


Fig.1 AFM phase images for SBR/NBR blends with 0.3, 0.5 and 0.7 of  $\phi_{\text{SBR}}$  prepared by spin coating from toluene (upper) and THF (lower) solutions.

Fig.2 shows the histogram analysis of AFM phase images for SBR/NBR blends with 0.3, 0.5 and 0.7 of  $\phi_{\text{SBR}}$  prepared from toluene and THF solutions. The phase difference corresponds to the energy absorption during one oscillation cycle of cantilever. The higher value of phase difference indicates the higher energy absorption part, i.e. SBR rich phase. The histogram showed two or three peaks depending on the  $\phi_{\text{SBR}}$  and the solvent used for the sample preparation. The peak observed at the highest phase difference was assigned to SBR rich phase, and the histogram peaks were analyzed by the numerical fitting using Gaussian function then the SBR fraction ( $\phi_{\text{SBR}}^*$ ) was evaluated. For the

histogram analysis, five AFM phase images observed at different locations for each SBR/NBR blend were used. The  $\phi_{\text{SBR}}^*$  value, which was evaluated by the histogram analysis for SBR/NBR blends prepared from THF solution, was smaller than  $\phi_{\text{SBR}}$ , however, the  $\phi_{\text{SBR}}^*$  value was larger than  $\phi_{\text{SBR}}$  for SBR/NBR blends prepared from toluene solution. These facts indicated that some part of NBR dissolved in SBR rich phase in toluene solution, and in contrast, SBR dissolved slightly in NBR rich phase in THF solution.

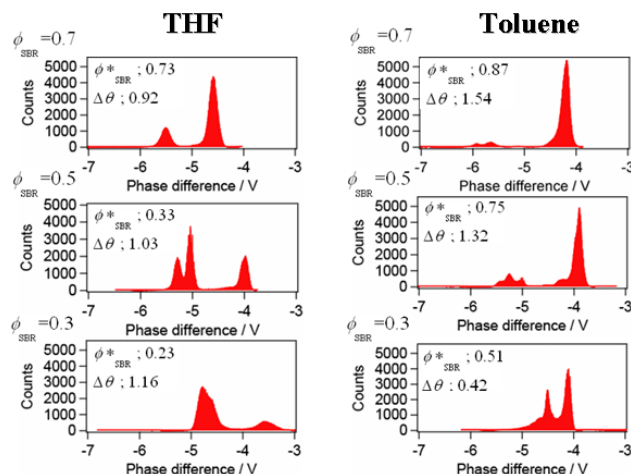


Fig.2 Histogram analysis for AFM phase images of SBR/NBR blends with 0.3, 0.5 and 0.7 of  $\phi_{\text{SBR}}$  prepared from toluene and THF solutions.

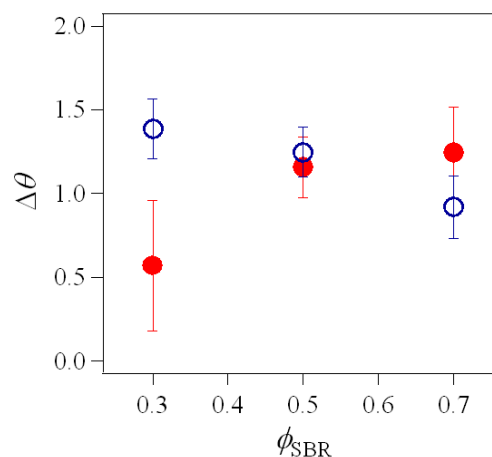


Fig.3 Relative change of phase angle difference between SBR rich and NBR rich phases against  $\phi_{\text{SBR}}$  for SBR/NBR blends prepared from toluene (solid circle) and THF (open circle) solution.

The peak at the lowest phase difference was assigned to the stiff NBR rich phase, the difference between the phase difference values of two peaks corresponding to NBR rich and SBR rich phases indicated the relative phase angle difference between NBR rich and SBR rich phases ( $\Delta\theta$ ). The obtained  $\Delta\theta$  was superimposed on each histogram in Fig.2. The average  $\Delta\theta$  values evaluated on five AFM phase images were plotted against  $\phi_{\text{SBR}}$  for SBR/NBR blends prepared from toluene and THF solutions in Fig.3. For SBR/NBR blend prepared from toluene solutions, the  $\Delta\theta$  value increased with the increase of  $\phi_{\text{SBR}}$ , however, SBR/NBR blends prepared from THF solutions showed the opposite tendency. The smaller the  $\Delta\theta$  values, the

composition difference between the SBR rich phase and the NBR rich phase became smaller, in other word, the Gibbs free energy of mixing ( $\Delta G_{\text{mix}}$ ) of the system decreased. Therefore Fig.3 indicates that the mixing state of SBR and NBR depends on  $\phi_{\text{SBR}}$  and the solvent used for the mixing.

A typical line profile analysis on an AFM phase image of SBR/NBR ( $\phi_{\text{SBR}} = 0.5$ ) prepared from toluene solution is shown in Fig. 4. Two types of NBR rich domain with diameter above 10 and less than 3  $\mu\text{m}$  were categorized in a SBR rich matrix. Any part of the SBR rich matrix and NBR rich domains showed constant voltages corresponding to the phase angles, however, the voltages changed continuously in between the SBR rich matrix and the NBR rich domains. This continuous change of the voltage was observed at any border between SBR rich matrix and NBR rich domains for both large and small domains. The interface thickness was evaluated from these voltage changed regions between SBR rich matrix and NBR rich domains. The size of NBR rich domains and SBR rich matrix was evaluated by measuring the constant voltage distance. From the line profile analysis of AFM phase images, the size of three phases, matrix, domain and interface, were obtained.

The line profile analysis was carried out by drawing a line perpendicular to the interface between a SBR rich matrix and a NBR rich domain. About 20 individual domains of diameter below 3  $\mu\text{m}$  and above 10  $\mu\text{m}$  were used for the line profile analysis. At least two lines profile analysis was carried out for each small domain, and then the average thickness of interface was evaluated. The shapes of the line profiles at the opposite boundary of NBR rich domains were symmetrical for both large and small domains.

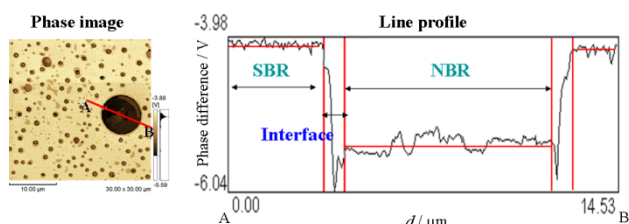


Fig.4 AFM phase image and line profile analysis for SBR/NBR blend with  $\phi_{\text{SBR}} = 0.5$  prepared from toluene solution.

The interface thicknesses are plotted against  $\phi_{\text{SBR}}$  for the small and large domains with the diameter less than 3  $\mu\text{m}$  and above 10  $\mu\text{m}$  in Fig.5. For the small domains less than 3  $\mu\text{m}$ , the average interface thickness was almost same for all  $\phi_{\text{SBR}}$ , 0.18  $\mu\text{m}$  for blends prepared from THF and 0.23  $\mu\text{m}$  for blends prepared from toluene solutions. In the large domains above 10  $\mu\text{m}$ , the interface thickness in SBR/NBR blends sample prepared by THF solution was almost the same for all  $\phi_{\text{SBR}}$ . The interface thickness of the SBR/NBR blends prepared from toluene decreased with increasing of  $\phi_{\text{SBR}}$ .

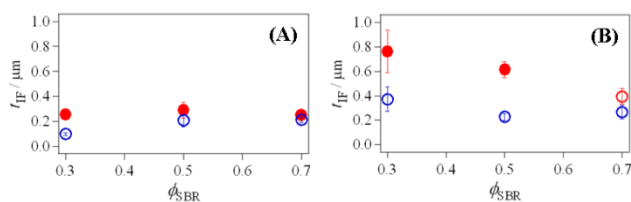


Fig.5 Relationship between the interface thickness and  $\phi_{\text{SBR}}$  for small domains ( $< 3 \mu\text{m}$ ) (A) and large domains ( $> 10 \mu\text{m}$ ) (B) of SBR/NBR blends prepared toluene (solid circle) and THF (open circle) solutions.

If the phase separated domain was assumed as a sphere of

radius  $r$ , the volume ratio of the interface against the domain was calculated as  $R(r) = t_{\text{IF}} 4\pi r^2 / \frac{4\pi r^3}{3} = 3t_{\text{IF}} / r$ . Here,  $t_{\text{IF}}$  is

the interface thickness evaluated by line profile analysis from AFM phase image. For the small domains, the experimental values were well described by this equation. However, the interface thickness of the larger domains was thicker than the value estimated by this equation. The small domains below 3  $\mu\text{m}$  always formed spherical domains for both SBR/NBR blends prepared from toluene and THF solutions. However, the large domains above 10  $\mu\text{m}$  showed not only non-spherical domains but also thicker interface than the value expected from the coagulation of the smaller domains.

### 3.2 DSC observation

Fig. 6 shows DSC heat flows for SBR, NBR and those blends with 0.5 of  $\phi_{\text{SBR}}$  prepared from THF solution. SBR and NBR showed one glass transition, however SBR/NBR blend showed two individual glass transitions at the same temperature region of SBR and NBR. The glass transition temperature ( $T_g$ ) and the heat capacity jump at  $T_g$  ( $\Delta C_p$ ) of neat SBR and NBR were 216 K ( $T_g^*_{\text{SBR}}$ ), 0.41 J/g ( $\Delta C_p^*_{\text{SBR}}$ ), and 238.8 K ( $T_g^*_{\text{NBR}}$ ), 0.49 J/g ( $\Delta C_p^*_{\text{NBR}}$ ), respectively. For the blend with 0.5 of  $\phi_{\text{SBR}}$ ,  $T_g$  and  $\Delta C_p$  for SBR domain and NBR matrix were 214.2 K ( $T_{g\text{SBR}}$ ), 0.18 J/g ( $\Delta C_{p\text{SBR}}$ ), and 238.2 K ( $T_{g\text{NBR}}$ ), 0.21 J/g ( $\Delta C_{p\text{NBR}}$ ), respectively. From the  $\Delta C_p$  value of NBR ( $\Delta C_p^*_{\text{NBR}}$ ), SBR ( $\Delta C_p^*_{\text{SBR}}$ ) and the blends ( $\Delta C_{p\text{NBR}}$ ,  $\Delta C_{p\text{SBR}}$ ), the weight fraction of NBR matrix ( $\phi^*_{\text{NBR}}$ ), SBR domain ( $\phi^*_{\text{SBR}}$ ) and the partial weight fraction of NBR ( $\phi^*_{\text{F NBR}}$ ) and SBR ( $\phi^*_{\text{F SBR}}$ ) in the interface for the blends were obtained as the following equation.

$$\begin{aligned} & \phi^*_{\text{NBR}} + \phi^*_{\text{IF NBR}} + \phi^*_{\text{SBR}} + \phi^*_{\text{IF SBR}} \\ &= (1 - \phi^*_{\text{SBR}}) \left\{ \frac{\Delta C_{p\text{NBR}}}{(1 - \phi^*_{\text{SBR}}) \Delta C_p^*_{\text{NBR}}} + \left[ 1 - \frac{\Delta C_{p\text{NBR}}}{(1 - \phi^*_{\text{SBR}}) \Delta C_p^*_{\text{NBR}}} \right] \right\} \\ &+ \phi^*_{\text{SBR}} \left\{ \frac{\Delta C_{p\text{SBR}}}{\phi^*_{\text{SBR}} \Delta C_p^*_{\text{SBR}}} + \left[ 1 - \frac{\Delta C_{p\text{SBR}}}{\phi^*_{\text{SBR}} \Delta C_p^*_{\text{SBR}}} \right] \right\} \\ &= 1 \end{aligned} \quad (1)$$

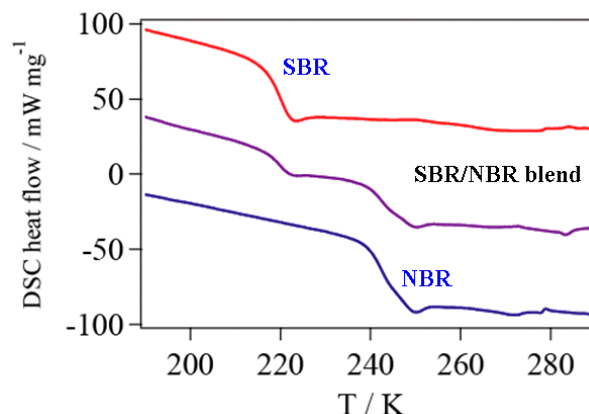


Fig.6 DSC heating curve for SBR, NBR and SBR/NBR blend with 0.5 of  $\phi_{\text{SBR}}$  prepared from THF solution.

From the DSC measurement, the partial weight fraction of NBR ( $\phi^*_{\text{F NBR}}$ ) and SBR ( $\phi^*_{\text{F SBR}}$ ) in the interface was evaluated for each SBR/NBR blends. The weight fractions of interface evaluated by DSC ( $\phi^*_I$ ) were obtained as  $\phi^*_I = \phi^*_{\text{F SBR}}$

+  $\phi_{IF}^* NBR$ , and plotted for each solvent used for the mixing in Fig. 7 (A). The interface thicknesses evaluated by the line profile analysis of AFM phase images for the large domains are also shown in Fig. 7 (B). The interface fraction evaluated from DSC and the interface thickness evaluated by AFM showed the same tendency for the blends at 0.3 and 0.7 of  $\phi_{SBR}$ , however, the blend at 0.5 of  $\phi_{SBR}$  showed opposite tendency. These results agreed with the results shown in Fig. 3. The SBR fractions evaluated by the histogram analysis,  $\phi_{SBR}^*$ , were larger than  $\phi_{SBR}$  of the blends prepared from toluene solutions. The mixing state of the blends depended on not only the solvent but also  $\phi_{SBR}$ . As shown in Fig. 3, the mixing state of SBR and NBR in the blend at 0.3 of  $\phi_{SBR}$  prepared from toluene solution was more miscible than that of the blend at the same  $\phi_{SBR}$  prepared from THF. On the other hand, the mixing state of blend at 0.5 of  $\phi_{SBR}$  prepared from either solvent was almost the same. The mixing state of the blend at 0.7 of  $\phi_{SBR}$  prepared from a THF solution became better than that of the blend prepared from a toluene solution.

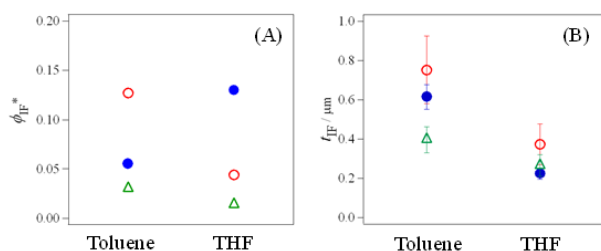


Fig.7 Weight fraction of interface evaluated by DSC (A) and the interface thickness for the large domains by AFM line profile analysis (B) for SBR/NBR blends prepared by different solvents with  $\phi_{SBR} = 0.3$  (open circle), 0.5 (solid circle), 0.7 (open triangle)..

The phase separation structures and the compositions of separated phases are influenced by the mixing state of the solutions and the phase separation process during the spin-coating. The compositions of SBR and NBR of the blends in THF and toluene solutions are shown in Table 1. The solutions were slowly and clearly phase separated after the mixing. The upper layer was SBR rich solution and the lower layer was NBR rich solution due to the bulk density difference between SBR (0.94 g/cm<sup>3</sup>) and NBR (0.98 g/cm<sup>3</sup>). The polymers' ratio (S/N) of each SBR rich and NBR rich layers in THF solution was almost the same regardless of  $\phi_{SBR}$ , however, the ratio of SBR rich and NBR rich layers in toluene solution was much higher especially in the SBR rich phase. In addition, the SBR rich solution layer is occupied much amount of toluene (0.7 to 0.8) independent of  $\phi_{SBR}$ . This suggests that SBR molecules well expanded in toluene solution and were difficult to coagulate during the spin-coating process. Therefore, any of the SBR/NBR blends prepared from toluene solutions showed SBR rich matrices.

Considering the solubility parameter difference between solvents and polymers,  $(\delta_s - \delta_r)^2$ , toluene was a good solvent of SBR,  $(\delta_s - \delta_r)^2 = 1.2 \text{ MPa}^{1/2}$ , than THF  $(\delta_s - \delta_r)^2 = 1.6 \text{ MPa}^{1/2}$ , and THF was a good solvent of NBR,  $(\delta_s - \delta_r)^2 = 1.3 \text{ MPa}^{1/2}$ , than toluene  $(\delta_s - \delta_r)^2 = 1.7 \text{ MPa}^{1/2}$ .

SBR/NBR ratio in the solid state prepared from the upper and lower solution layers indicated that the composition difference between SBR rich phase and NBR rich phase became small with the increase of  $\phi_{SBR}$  in the blend prepared from THF solution. On the other hand, the composition difference became larger

with the increase of  $\phi_{SBR}$  in the blend prepared from toluene solution. These facts show a good agreement with the results shown in Fig. 3. These facts indicated that the composition of SBR rich and NBR rich phase in solutions were kept in SBR/NBR blends after spin-coating. As described above, the matrix changed from NBR rich phase to SBR rich phase for SBR/NBR blend prepared from THF solution at 0.5 of  $\phi_{SBR}$ , because the SBR/NBR ratio in the upper SBR rich layer became closer to the NBR/SBR ratio in the lower NBR rich layer. In toluene solution, SBR molecules expanded by swelling of toluene in the upper layer, and the mixing state of SBR and NBR in the lower layer of toluene solution was better than that in THF solution. This better mixing state of SBR and NBR formed the thick interface in the solid SBR/NBR blends prepared from toluene solution.

Table 1 Composition of phase separation layers in SBR/NBR solution

$\phi_{SBR}$	SBR rich phase* <sup>1</sup>				NBR rich phase* <sup>2</sup>			
	THF	SBR	NBR	S/N* <sup>3</sup>	THF	SBR	NBR	S/N* <sup>3</sup>
0.3	0.158	0.006	0.002	3	0.794	0.010	0.030	0.33
0.5	0.547	0.021	0.008	2.6	0.405	0.005	0.014	0.36
0.7	0.685	0.029	0.008	3.6	0.265	0.003	0.010	0.3

$\phi_{SBR}$	SBR rich phase* <sup>1</sup>				NBR rich phase* <sup>2</sup>			
	Tolu	SBR	NBR	S/N* <sup>3</sup>	Tolu	SBR	NBR	S/N* <sup>3</sup>
0.3	0.741	0.021	0.001	21	0.220	0.007	0.010	0.7
0.5	0.718	0.024	0.001	24	0.239	0.005	0.013	0.38
0.7	0.799	0.030	0.005	6	0.157	0.002	0.007	0.29

\*1 Upper layer

\*2 Lower layer

\*3 SBR/NBR fraction ratio in the solid obtained by solvent casting evaluated by FTIR method

## 4. Conclusions

The phase separation structure and the interface of SBR/NBR blends prepared from toluene and THF solutions were investigated by AFM and DSC. The thickness of interface between SBR rich and NBR rich phases was determined by the line profile analysis of AFM phase images. The interface thickness of SBR/NBR blend prepared from toluene solution was thicker than that of the blend prepared from THF. The maximum thickness of interface was observed at  $\phi_{SBR} = 0.3$  prepared from toluene solution. And the interface thickness also depended on the size of phase separated domains. These results suggested that the mixing state of SBR and NBR molecules in each solvent and the phase separating process influenced the thickness of the interfaces. The volume fraction of interface was evaluated from the heat capacity jump at glass transition of SBR and NBR by DSC. The interface volume fraction and the interface thickness evaluated showed the same tendency for the blends with 0.3 and 0.7 of  $\phi_{SBR}$ , however, the results of the blend with 0.5 of  $\phi_{SBR}$  showed the opposite tendency due to the small difference of mixing state between toluene and THF solutions.

## References

- 1) S. H. Botros, A. F. Moustafa, S. A. Ibrahim, *J. Appl. Polym. Sci.* **99**, 1559 (2006).
- 2) M. Kawazoe, H. Ishida, *Macromolecules* **41**, 2931 (2008).
- 3) M. Kawazoe, H. Ishida, *Macromolecules* **42**, 6175 (2009).

- 4) E. H. Andrews, *J. Roy. Microscop. Soc.*, **82**, 221-223 (1964)
- 5) S. Koizumi, H. Hasegawa, T. Hashimoto, *Macromolecules*, **27**, 7893 (1994)
- 6) T. Koga, T. Hashimoto, M. Takenaka, K. Aizawa, N. Amino, M. Nakamura, D. Yamaguchi, S. Koizumi, *Macromolecules*, **41**, 453 (2008)
- 7) H. Sasaki, P. K. Bala, H. Yoshida, *Polymer*, **25**, 4805 (1995)
- 8) D. J. Hourston, M. Song, *J. Appl. Polym. Sci.*, **76**, 1791 (2000)